A Reduced-Complexity Multiband MIMO Receiver with Estimation of Analog Devices Imperfection

Tomoya Ohta and Masahiro Morikura
Graduate School of Informatics, Kyoto University
Yoshida-honmachi, Sakyo-ku, Kyoto 606-8501, Japan
Email: ohta@imc.cce.i.kyoto-u.ac.jp

Satoshi Denno
Graduate School of Natural Science and Technology,
Okayama University
3-1-1 Tsushima-naka, Kita-ku, Okayama 700-8530, Japan

***Abstract*—Cognitive radios are of interest because they are capable of high frequency utilization efficiency. Multiband multiple-input multiple-output (MIMO) receivers based on heterodyne reception have been proposed for use in cognitive radios. This paper proposes a reduced-complexity multiband MIMO receiver that can achieve high performance by correcting the imperfection of the Hilbert transformer in the intermediate frequency (IF) band. However, the imperfection of the analog devices in the feedback loop causes poor performance. Therefore, a scheme for correcting the imperfection of the analog devices is proposed.**

I. INTRODUCTION

The number of subscribers to cellular communication systems is still increasing in the world. In addition to cellular systems, short-range wireless communication systems such as wireless local area networks (WLANs) accommodate many users. Because the frequency spectrum available for radio communication is limited, it is necessary to raise the frequency utilization efficiency to accommodate this growing number of users. Cognitive radios are of interest because they are capable of high frequency utilization efficiency. The technology used in these radios involves the use of frequency bands even if they are temporarily empty [1], [2]. In cognitive radios, multiband receivers with only one frequency conversion chain are necessary to miniaturize the receivers. Because the pass bands of the band-pass filter (BPF) in the radio frequency (RF) stage must be wider than usual in order to cope with signals in several frequency bands [3], the heterodyne receiver for multiband reception suffers from image-band interference [4]. In principle, this interference can be canceled by introducing a Hilbert transformer in the RF stage [5]. However, the image-band interference cannot be suppressed perfectly, because the Hilbert transformer is imperfect. Therefore, it is necessary to correct the imperfection of the Hilbert transformer.

Multiple-input multiple-output (MIMO) spatial multiplexing is used to increase the frequency utilization efficiency by using multiple antennas in the transmitter and receiver [6], [7]. In fact, a multiband MIMO receiver with ordered successive detection (OSD) has been proposed [8]. However, the imperfection of the Hilbert transformer has only been corrected in the baseband.

In this paper, the imperfection is corrected in the intermediate frequency (IF) band to reduce the receiver's complexity. However, the imperfection of the analog devices in the feedback loop causes poor performance. Therefore, a scheme for correcting the imperfection of the analog devices is proposed.

II. SYSTEM MODEL

The system model is shown in Fig. 1. In a MIMO system with N_{T} antennas in the transmitter and N_{R} antennas in the receiver, a QPSK signal is transmitted by using a quadrature modulator. Then, the n-th received signal is down-converted from the RF band to the IF band by the Hilbert transformer implemented with analog devices. Since the analog Hilbert transformer is imperfect, the imperfection should be corrected in the IF stage following the Hilbert transformer, as illustrated in Fig. 1. The corrected signal is fed to two complex down-converters (called "dual frequency converters") [9]. In one converter, the desired signal is down-converted into the baseband and the output is fed to a low-pass filter (LPF). In the other converter, the image-band interference is down-converted into the baseband and the output is also fed to a LPF. The two outputs of the LPFs are sampled by A/D converters. Therefore, the time index of the signals hereafter becomes discrete. The digitized baseband signals $\boldsymbol{y}_n(k) = \left(y_{\mathrm{D},n}(k)\ y^*_{\mathrm{I},n}(k)\right)^{\mathrm{T}}$ can be expressed in a complex vector form as follows, where the index T represents the transpose of a matrix or vector:

$$\boldsymbol{y}_n(k) = \begin{pmatrix} \beta_n & \alpha_n \\ \alpha^*_n & \beta^*_n \end{pmatrix} \begin{pmatrix} r_{\mathrm{D},n}(k) \\ r^*_{\mathrm{I},n}(k) \end{pmatrix} = G_{\mathrm{BB},n} \begin{pmatrix} r_{\mathrm{D},n}(k) \\ r^*_{\mathrm{I},n}(k) \end{pmatrix}. \quad (1)$$

In (1), $*$ denotes the complex conjugate. In addition, the baseband signals $r_{\mathrm{D},n}(k)$ and $r_{\mathrm{I},n}(k)$ are defined as

$$r_{\mathrm{D},n}(k) = \sum_{i=1}^{N_{\mathrm{T}}} h_{\mathrm{D},n,i}(k) x_{\mathrm{D},i}(k) + n_{\mathrm{D},n}(k) \quad (2)$$

$$r_{\mathrm{I},n}(k) = \sum_{i=1}^{N_{\mathrm{T}}} h_{\mathrm{I},n,i}(k) x_{\mathrm{I},i}(k) + n_{\mathrm{I},n}(k), \quad (3)$$

where $h_{\mathrm{D},n,i}(k)$, $x_{\mathrm{D},i}(k)$, and $n_{\mathrm{D},n}(k)$ represent the channel impulse response, the transmitted signal, and the additive white Gaussian noise (AWGN) of the desired side, respectively, and $h_{\mathrm{I},n,i}(k)$, $x_{\mathrm{I},i}(k)$, and $n_{\mathrm{I},n}(k)$ represent the channel impulse response, the transmitted signal, and the AWGN of the image-band side. On the other hand, the baseband gain matrix $G_{\mathrm{BB},n}$ is defined as

$$G_{\mathrm{BB},n} = \begin{pmatrix} \beta_n & \alpha_n \\ \alpha^*_n & \beta^*_n \end{pmatrix}, \quad (4)$$

978-1-4673-0990-5/12/$31.00

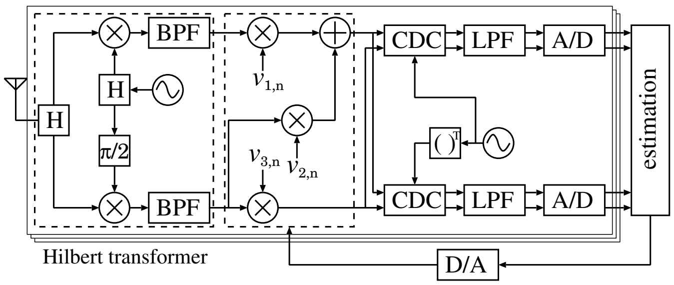

Fig. 1. System model.

where the complex coefficients α_n and β_n are defined as

$$\alpha_n = \frac{1}{4}\left\{v_{1,n} g_{\mathrm{I},n} e^{\mathrm{j}\phi_n} - (v_{3,n} - \mathrm{j}v_{2,n})\, g_{\mathrm{Q},n}\right\} \quad (5)$$

$$\beta_n = \frac{1}{4}\left\{v_{1,n} g_{\mathrm{I},n} e^{-\mathrm{j}\phi_n} + (v_{3,n} - \mathrm{j}v_{2,n})\, g_{\mathrm{Q},n}\right\}. \quad (6)$$

In (5) and (6), j, ϕ_n, $g_{\mathrm{I},n}$, and $g_{\mathrm{Q},n}$ represent the imaginary unit, the I/Q phase error, and the I and Q channel gains of the Hilbert transformer, respectively, and $v_{1,n}$, $v_{2,n}$, and $v_{3,n}$ represent the correction values.

III. Proposed Scheme for Correcting the Analog Devices Imperfection

A. Orthogonal Training Sequences

In our proposed scheme, orthogonal training sequences based on the Walsh code are used for training sequences. The Walsh code $c_i(l)$ has the following property:

$$\sum_{l=1}^{N_\mathrm{T}} c_i(l) c_m(l) = \begin{cases} N_\mathrm{T} & i = m \\ 0 & i \neq m \end{cases}. \quad (7)$$

By using the Walsh code, the training sequences transmitted from the i-th antenna can be expressed as

$$x_i\left(l + N_\mathrm{T}(k-1)\right) = c_i(l) d_i(k), \quad (8)$$

where $d_i(k)$ represents a BPSK signal whose value is ± 1.

B. Estimation of Hilbert Transformer Imperfection

When the estimation packet is received, the correction values $v_{1,n} = v_{3,n} = 1$ and $v_{2,n} = 0$ are assumed at first in order to simplify the system model. By multiplying the baseband signal vector $\boldsymbol{y}_n(k)$ and the Walsh code $c_i(l)$, the output $\boldsymbol{z}_{n,i}(k)$ can be written as

$$\boldsymbol{z}_{n,i}(k) = \sum_{l=1}^{N_\mathrm{T}} c_i(l) \begin{pmatrix} y_{\mathrm{D},n}\left(l + N_\mathrm{T}(k-1)\right) \\ y^*_{\mathrm{I},n}\left(l + N_\mathrm{T}(k-1)\right) \end{pmatrix}. \quad (9)$$

From the output $\boldsymbol{z}_{n,i}(k)$ in (9), the minimum mean square error (MMSE) weight vector $\boldsymbol{w}_{n,i} = \left(w^{(1)}_{n,i}\ w^{(2)}_{n,i}\right)^\mathrm{T}$ minimizing the cost function J is generated by the recursive least squares (RLS) algorithm [10]:

$$J = \mathrm{E}\left[\left|d_i(k) - \boldsymbol{w}^\mathrm{H}_{n,i}\boldsymbol{z}_{n,i}(k)\right|^2\right] \to \min, \quad (10)$$

where the index H represents the conjugate transpose of a matrix or vector. In (10), $\mathrm{E}[\cdot]$ denotes the ensemble average. The solution of (10) can be written as

$$\begin{aligned} \boldsymbol{w}_{n,i} &= \mathrm{E}\left[\boldsymbol{z}_{n,i}(k)\boldsymbol{z}^\mathrm{H}_{n,i}(k)\right]^{-1} \mathrm{E}\left[\boldsymbol{z}_{n,i}(k) d^*_i(k)\right] \\ &= \left(\left|N_\mathrm{T} h_{\mathrm{D},n,i}(k)\right|^2 + \frac{\sigma^2}{\sigma_x^2}\right)^{-1} \frac{N_\mathrm{T} h_{\mathrm{D},n,i}(k)}{|\beta_n|^2 - |\alpha_n|^2} \begin{pmatrix} \beta_n \\ -\alpha^*_n \end{pmatrix}. \end{aligned} \quad (11)$$

In (11), dividing the second element by the first element, $-\frac{\alpha^*_n}{\beta_n}$ can be estimated as

$$-\frac{\overline{\alpha}^*_n}{\overline{\beta}_n} = \frac{1}{N_\mathrm{T}} \sum_{i=1}^{N_\mathrm{T}} \frac{w^{(2)}_{n,i}}{w^{(1)}_{n,i}}. \quad (12)$$

Then, from (5) and (6) and using the $-\frac{\overline{\alpha}^*_n}{\overline{\beta}_n}$ estimation in (12), $\left(g_{\mathrm{I},n}/g_{\mathrm{Q},n}\right) e^{-\mathrm{j}\phi_n}$ can be estimated as

$$\frac{\overline{g}_{\mathrm{I},n}}{\overline{g}_{\mathrm{Q},n}} e^{-\mathrm{j}\overline{\phi}_n} = \frac{1 + \frac{\overline{\alpha}^*_n}{\overline{\beta}_n}}{1 - \frac{\overline{\alpha}^*_n}{\overline{\beta}_n}}. \quad (13)$$

In addition, the I/Q gain ratio $g_{\mathrm{I},n}/g_{\mathrm{Q},n}$ and the I/Q phase error ϕ_n can be estimated as

$$\frac{\overline{g}_{\mathrm{I},n}}{\overline{g}_{\mathrm{Q},n}} = \left|\frac{1 + \frac{\overline{\alpha}^*_n}{\overline{\beta}_n}}{1 - \frac{\overline{\alpha}^*_n}{\overline{\beta}_n}}\right| \quad (14)$$

$$\overline{\phi}_n = -\arctan\left(\frac{1 + \frac{\overline{\alpha}^*_n}{\overline{\beta}_n}}{1 - \frac{\overline{\alpha}^*_n}{\overline{\beta}_n}}\right). \quad (15)$$

Thus, the imperfection of the Hilbert transformer can be estimated.

C. Estimation of the Analog Devices Imperfection

Since the analog devices in the feedback loop are imperfect, we assume that the gains $\epsilon_{1,n}$, $\epsilon_{2,n}$, and $\epsilon_{3,n}$ and the DC-offsets $\delta_{1,n}$, $\delta_{2,n}$, and $\delta_{3,n}$ occur in the analog devices. Then, the correction values $v_{1,n}$, $v_{2,n}$, and $v_{3,n}$ can be expressed as

$$v_{1,n} = \epsilon_{1,n}\overline{v}_{1,n} + \delta_{1,n} \quad (16)$$

$$v_{2,n} = \epsilon_{2,n}\overline{v}_{2,n} + \delta_{2,n} \quad (17)$$

$$v_{3,n} = \epsilon_{3,n}\overline{v}_{3,n} + \delta_{3,n}, \quad (18)$$

where $\overline{v}_{1,n}$, $\overline{v}_{2,n}$, and $\overline{v}_{3,n}$ represent the inputs to the feedback loop for the correction. In this case, α_n in (5) and β_n in (6) can be rewritten as

$$\begin{aligned} \alpha_n = &\ \frac{1}{4}\left(\epsilon_{1,n}\overline{v}_{1,n} + \delta_{1,n}\right) g_{\mathrm{I},n} e^{\mathrm{j}\phi_n} \\ &- \frac{1}{4}\left(\epsilon_{3,n}\overline{v}_{3,n} + \delta_{3,n}\right) g_{\mathrm{Q},n} \\ &+ \mathrm{j}\frac{1}{4}\left(\epsilon_{2,n}\overline{v}_{2,n} + \delta_{2,n}\right) g_{\mathrm{Q},n} \end{aligned} \quad (19)$$

$$\begin{aligned} \beta_n = &\ \frac{1}{4}\left(\epsilon_{1,n}\overline{v}_{1,n} + \delta_{1,n}\right) g_{\mathrm{I},n} e^{-\mathrm{j}\phi_n} \\ &+ \frac{1}{4}\left(\epsilon_{3,n}\overline{v}_{3,n} + \delta_{3,n}\right) g_{\mathrm{Q},n} \\ &- \mathrm{j}\frac{1}{4}\left(\epsilon_{2,n}\overline{v}_{2,n} + \delta_{2,n}\right) g_{\mathrm{Q},n}. \end{aligned} \quad (20)$$

A scheme for correcting the imperfection of the analog devices in the feedback loop is described below.

When the estimation packet is received, by multiplying the baseband signal vector $\boldsymbol{y}_n(k)$ and the Walsh code $c_i(l)$, the output $\boldsymbol{z}_{n,i}(k)$ can be written as

$$\boldsymbol{z}_{n,i}(k) = \sum_{l=1}^{N_\mathrm{T}} c_i(l) \begin{pmatrix} y_{\mathrm{D},n}\left(l+N_\mathrm{T}(k-1)\right) \\ y_{\mathrm{I},n}^{*}\left(l+N_\mathrm{T}(k-1)\right) \end{pmatrix}. \tag{21}$$

From the output $\boldsymbol{z}_{n,i}(k)$ in (21), the MMSE weight vector $\boldsymbol{w}_{n,i} = \left(w_{n,i}^{(1)}\ w_{n,i}^{(2)}\right)^\mathrm{T}$ minimizing the cost function J is generated by the RLS algorithm:

$$J = \mathrm{E}\left[\left|d_i(k) - \boldsymbol{w}_{n,i}^\mathrm{H}\boldsymbol{z}_{n,i}(k)\right|^2\right] \to \min. \tag{22}$$

The solution of (22) can be written as

$$\begin{aligned} \boldsymbol{w}_{n,i} &= \mathrm{E}\left[\boldsymbol{z}_{n,i}(k)\boldsymbol{z}_{n,i}^\mathrm{H}(k)\right]^{-1}\mathrm{E}\left[\boldsymbol{z}_{n,i}(k)d_i^{*}(k)\right] \\ &= \left(\left|N_\mathrm{T}h_{\mathrm{D},n,i}(k)\right|^2 + \frac{\sigma^2}{\sigma_x^2}\right)^{-1} \frac{N_\mathrm{T}h_{\mathrm{D},n,i}(k)}{|\beta_n|^2 - |\alpha_n|^2}\begin{pmatrix}\beta_n \\ -\alpha_n^{*}\end{pmatrix}. \end{aligned} \tag{23}$$

Then, λ_n is defined as

$$\lambda_n = \frac{1}{N_\mathrm{T}}\sum_{i=1}^{N_\mathrm{T}} \frac{w_{n,i}^{(2)}}{w_{n,i}^{(1)}} = -\frac{\alpha_n^{*}}{\beta_n}. \tag{24}$$

Using (19) and (20), this equation can be rewritten as

$$\begin{aligned} &a_{1,n}\epsilon_{1,n} + a_{2,n}\epsilon_{2,n} + a_{3,n}\epsilon_{3,n} \\ &+ b_{1,n}\delta_{1,n} + b_{2,n}\delta_{2,n} + b_{3,n}\delta_{3,n} = 0, \end{aligned} \tag{25}$$

where $a_{1,n}$, $a_{2,n}$, $a_{3,n}$, $b_{1,n}$, $b_{2,n}$, and $b_{3,n}$ can be expressed as follows:

$$a_{1,n} = (\lambda_n + 1)\,\overline{v}_{1,n}g_{\mathrm{I},n}e^{-\mathrm{j}\phi_n} \tag{26}$$

$$a_{2,n} = -\mathrm{j}\,(\lambda_n + 1)\,\overline{v}_{2,n}g_{\mathrm{Q},n} \tag{27}$$

$$a_{3,n} = (\lambda_n - 1)\,\overline{v}_{3,n}g_{\mathrm{Q},n} \tag{28}$$

$$b_{1,n} = (\lambda_n + 1)\,g_{\mathrm{I},n}e^{-\mathrm{j}\phi_n} \tag{29}$$

$$b_{2,n} = -\mathrm{j}\,(\lambda_n + 1)\,g_{\mathrm{Q},n} \tag{30}$$

$$b_{3,n} = (\lambda_n - 1)\,g_{\mathrm{Q},n}. \tag{31}$$

By setting $x_n = \delta_{1,n} + K_n\delta_{2,n}$, (25) can be rewritten as

$$a_{1,n}\epsilon_{1,n} + a_{2,n}\epsilon_{2,n} + a_{3,n}\epsilon_{3,n} + b_{1,n}x_n + b_{3,n}\delta_{3,n} = 0 \tag{32}$$

$$K_n = \frac{b_{2,n}}{b_{1,n}} = -\mathrm{j}\frac{g_{\mathrm{Q},n}}{g_{\mathrm{I},n}}e^{\mathrm{j}\phi_n}. \tag{33}$$

From the four patterns of equations in (32) generated by changing the setting of the correction values, the following simultaneous equations can be obtained as

$$\begin{pmatrix} a_{2,n}^{(1)} & a_{3,n}^{(1)} & b_{1,n}^{(1)} & b_{3,n}^{(1)} \\ a_{2,n}^{(2)} & a_{3,n}^{(2)} & b_{1,n}^{(2)} & b_{3,n}^{(2)} \\ a_{2,n}^{(3)} & a_{3,n}^{(3)} & b_{1,n}^{(3)} & b_{3,n}^{(3)} \\ a_{2,n}^{(4)} & a_{3,n}^{(4)} & b_{1,n}^{(4)} & b_{3,n}^{(4)} \end{pmatrix} \begin{pmatrix} \hat{\epsilon}_{2,n} \\ \hat{\epsilon}_{3,n} \\ \hat{x}_n \\ \hat{\delta}_{3,n} \end{pmatrix} = -\begin{pmatrix} a_{1,n}^{(1)} \\ a_{1,n}^{(2)} \\ a_{1,n}^{(3)} \\ a_{1,n}^{(4)} \end{pmatrix}, \tag{34}$$

where $\hat{\epsilon}_{2,n} = \epsilon_{2,n}/\epsilon_{1,n}$, $\hat{\epsilon}_{3,n} = \epsilon_{3,n}/\epsilon_{1,n}$, $\hat{x}_n = x_n/\epsilon_{1,n}$, and $\hat{\delta}_{3,n} = \delta_{3,n}/\epsilon_{1,n}$.

By solving the simultaneous equations in (34), $\hat{\epsilon}_{2,n}$, $\hat{\epsilon}_{3,n}$, $\hat{x}_n$, and $\hat{\delta}_{3,n}$ can be obtained. Letting the real part of $\hat{x}_n$ be $\hat{x}_{n,\mathrm{Re}}$, the imaginary part be $\hat{x}_{n,\mathrm{Im}}$, $\hat{\delta}_{1,n} = \delta_{1,n}/\epsilon_{1,n}$, and $\hat{\delta}_{2,n} = \delta_{2,n}/\epsilon_{1,n}$, since $\hat{\delta}_{1,n}$ and $\hat{\delta}_{2,n}$ are real numbers and $\hat{x}_n = \hat{x}_{n,\mathrm{Re}} + \mathrm{j}\hat{x}_{n,\mathrm{Im}} = \hat{\delta}_{1,n} + K_n\hat{\delta}_{2,n}$, the following equation is formed:

$$\begin{pmatrix} \hat{x}_{n,\mathrm{Re}} \\ \hat{x}_{n,\mathrm{Im}} \end{pmatrix} = \begin{pmatrix} 1 & \frac{g_{\mathrm{Q},n}}{g_{\mathrm{I},n}}\sin\phi_n \\ 0 & -\frac{g_{\mathrm{Q},n}}{g_{\mathrm{I},n}}\cos\phi_n \end{pmatrix} \begin{pmatrix} \hat{\delta}_{1,n} \\ \hat{\delta}_{2,n} \end{pmatrix}. \tag{35}$$

Therefore, $\hat{\delta}_{1,n}$ and $\hat{\delta}_{2,n}$ can be obtained as

$$\begin{aligned} \begin{pmatrix} \hat{\delta}_{1,n} \\ \hat{\delta}_{2,n} \end{pmatrix} &= \begin{pmatrix} 1 & \frac{g_{\mathrm{Q},n}}{g_{\mathrm{I},n}}\sin\phi_n \\ 0 & -\frac{g_{\mathrm{Q},n}}{g_{\mathrm{I},n}}\cos\phi_n \end{pmatrix}^{-1} \begin{pmatrix} \hat{x}_{n,\mathrm{Re}} \\ \hat{x}_{n,\mathrm{Im}} \end{pmatrix} \\ &= \begin{pmatrix} 1 & \tan\phi_n \\ 0 & -\frac{g_{\mathrm{I},n}}{g_{\mathrm{Q},n}\cos\phi_n} \end{pmatrix} \begin{pmatrix} \hat{x}_{n,\mathrm{Re}} \\ \hat{x}_{n,\mathrm{Im}} \end{pmatrix}. \end{aligned} \tag{36}$$

Since $\hat{\epsilon}_{2,n}$, $\hat{\epsilon}_{3,n}$, $\hat{\delta}_{1,n}$, $\hat{\delta}_{2,n}$, and $\hat{\delta}_{3,n}$ have been estimated, $\epsilon_{1,n}$ can be estimated in the next step. Here, (23) can be rewritten as

$$\boldsymbol{w}_{n,i} = \begin{pmatrix} w_{n,i}^{(1)} \\ w_{n,i}^{(2)} \end{pmatrix} = \frac{1}{\epsilon_{1,n}} \begin{pmatrix} \hat{w}_{n,i}^{(1)} \\ \hat{w}_{n,i}^{(2)} \end{pmatrix}, \tag{37}$$

where $\hat{\boldsymbol{w}}_{n,i} = \left(\hat{w}_{n,i}^{(1)}\ \hat{w}_{n,i}^{(2)}\right)^\mathrm{T}$ is expressed as

$$\hat{\boldsymbol{w}}_{n,i} = \begin{pmatrix} \hat{w}_{n,i}^{(1)} \\ \hat{w}_{n,i}^{(2)} \end{pmatrix} = \hat{Q}_n \begin{pmatrix} \hat{\beta}_n \\ -\hat{\alpha}_n^{*} \end{pmatrix} \tag{38}$$

$$\hat{Q}_n = \frac{4\left(\left|N_\mathrm{T}h_{\mathrm{D},n,i}(k)\right|^2 + \frac{\sigma^2}{\sigma_x^2}\right)^{-1} N_\mathrm{T}h_{\mathrm{D},n,i}(k)}{g_{\mathrm{I},n}g_{\mathrm{Q},n}\cos\phi_n\left(\overline{v}_{1,n} + \hat{\delta}_{1,n}\right)\left(\hat{\epsilon}_{3,n}\overline{v}_{3,n} + \hat{\delta}_{3,n}\right)} \tag{39}$$

$$\begin{aligned} \hat{\alpha}_n &= \frac{1}{4}\left(\overline{v}_{1,n} + \hat{\delta}_{1,n}\right)g_{\mathrm{I},n}e^{\mathrm{j}\phi_n} \\ &\quad - \frac{1}{4}\left(\hat{\epsilon}_{3,n}\overline{v}_{3,n} + \hat{\delta}_{3,n}\right)g_{\mathrm{Q},n} \\ &\quad + \mathrm{j}\frac{1}{4}\left(\hat{\epsilon}_{2,n}\overline{v}_{2,n} + \hat{\delta}_{2,n}\right)g_{\mathrm{Q},n} \end{aligned} \tag{40}$$

$$\begin{aligned} \hat{\beta}_n &= \frac{1}{4}\left(\overline{v}_{1,n} + \hat{\delta}_{1,n}\right)g_{\mathrm{I},n}e^{-\mathrm{j}\phi_n} \\ &\quad + \frac{1}{4}\left(\hat{\epsilon}_{3,n}\overline{v}_{3,n} + \hat{\delta}_{3,n}\right)g_{\mathrm{Q},n} \\ &\quad - \mathrm{j}\frac{1}{4}\left(\hat{\epsilon}_{2,n}\overline{v}_{2,n} + \hat{\delta}_{2,n}\right)g_{\mathrm{Q},n}. \end{aligned} \tag{41}$$

Accordingly, from the MMSE weight vector $\boldsymbol{w}_{n,i}$ generated by the RLS algorithm and $\hat{\boldsymbol{w}}_{n,i}$ calculated theoretically by using the estimation results, $\epsilon_{1,n}$ can be estimated as

$$\epsilon_{1,n} = \frac{1}{2}\left(\frac{\hat{w}_{n,i_\mathrm{max}}^{(1)}}{w_{n,i_\mathrm{max}}^{(1)}} + \frac{\hat{w}_{n,i_\mathrm{max}}^{(2)}}{w_{n,i_\mathrm{max}}^{(2)}}\right). \tag{42}$$

In (42), when $\left|h_{\mathrm{D},n,i}(k)\right|^2$ is maximized, $i = i_\mathrm{max}$.

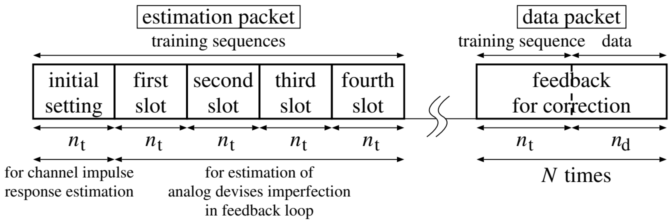

Fig. 2. Packet structure.

Since $\epsilon_{1,n}$ has been estimated, $\epsilon_{2,n}$, $\epsilon_{3,n}$, $\delta_{1,n}$, $\delta_{2,n}$, and $\delta_{3,n}$ can be estimated by multiplying $\hat{\epsilon}_{2,n}$, $\hat{\epsilon}_{3,n}$, $\hat{\delta}_{1,n}$, $\hat{\delta}_{2,n}$, and $\hat{\delta}_{3,n}$ by $\epsilon_{1,n}$. From these estimation results, the imperfection of the Hilbert transformer and the imperfection of the analog devices can be corrected simultaneously by calculating the correction values $\overline{v}_{1,n}$, $\overline{v}_{2,n}$, and $\overline{v}_{3,n}$ as follows in the baseband and providing them to the feedback loop:

$$\overline{v}_{1,n} = \frac{1}{\overline{\epsilon}_{1,n}} \left(\frac{1}{\overline{g}_{\mathrm{I},n} \cos \overline{\phi}_n} - \overline{\delta}_{1,n} \right) \tag{43}$$

$$\overline{v}_{2,n} = \frac{1}{\overline{\epsilon}_{2,n}} \left(-\frac{1}{\overline{g}_{\mathrm{Q},n}} \tan \overline{\phi}_n - \overline{\delta}_{2,n} \right) \tag{44}$$

$$\overline{v}_{3,n} = \frac{1}{\overline{\epsilon}_{3,n}} \left(\frac{1}{\overline{g}_{\mathrm{Q},n}} - \overline{\delta}_{3,n} \right). \tag{45}$$

D. Correction Value Settings

To solve the simultaneous equations in (34) (in the case that the coefficient matrix is a regular matrix), it is necessary to set the correction values properly. For example, when $\overline{v}_{1,n} = \overline{v}_{2,n} = \overline{v}_{3,n} = 1$ in the first slot, $\overline{v}_{1,n} = \overline{v}_{3,n} = 1$ and $\overline{v}_{2,n} = 0$ in the second slot, $\overline{v}_{1,n} = 1$ and $\overline{v}_{2,n} = \overline{v}_{3,n} = 0$ in the third slot, and $\overline{v}_{1,n} = \overline{v}_{2,n} = 0$ and $\overline{v}_{3,n} = 1$ in the fourth slot, the solution of the simultaneous equations exists. In this case, the correction value settings are expressed as $(1,1,1),(1,0,1),(1,0,0),(0,0,1)$.

The packet structure is shown in Fig. 2. First, the training sequences are transmitted only one time, and the imperfection of the Hilbert transformer, the channel impulse response, and the imperfection of the analog devices are estimated. Then, the data sequences are transmitted N times. Although the initial stage is complex, the others have reduced complexity, and one side of the two complex down-converters can be stopped.

IV. Simulation Results

This section discusses the performance of the proposed receiver, which was evaluated by performing computer simulation. The simulation parameters are listed in Tab. I. In the simulations, the Hilbert transformer is assumed to have an equal imperfection of $g_{\mathrm{I},n}/g_{\mathrm{Q},n} = 0.90$ and $\phi_n = \pi/18$ for every array, and the analog devices are also assumed to have an equal imperfection of $\epsilon_{1,n} = \epsilon_{2,n} = \epsilon_{3,n} = 0.90$ and $\delta_{1,n} = \delta_{2,n} = \delta_{3,n} = 0.10$ for every array, for simplicity. Moreover, it is assumed that the estimation of the channel impulse response is perfect and that the proposed receiver makes use of OSD.

TABLE I
Simulation parameters.

Parameters	Value
Modulation	QPSK
Channel Model	Rayleigh Fading
Noise	Additive White Gaussian Noise
Packet Size	500 Symbols
n_t	100 Symbols
(N_T,N_R)	(4,4)

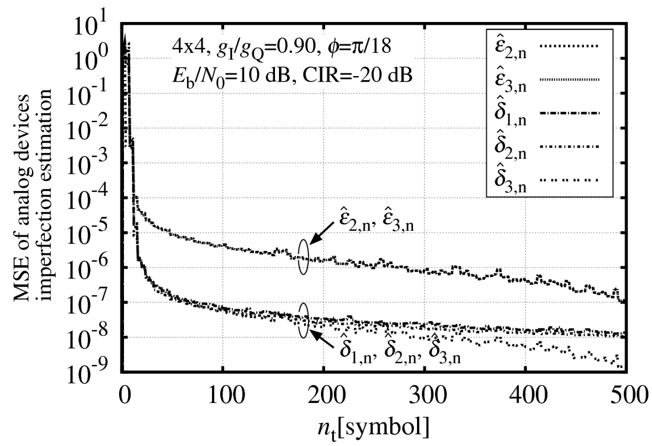

Fig. 3. Convergence property of $\hat{\epsilon}_{2,n}$, $\hat{\epsilon}_{3,n}$, $\hat{\delta}_{1,n}$, $\hat{\delta}_{2,n}$, and $\hat{\delta}_{3,n}$ estimation.

A. Estimation Performance of the Analog Devices Imperfection

The convergence properties of $\hat{\epsilon}_{2,n}$, $\hat{\epsilon}_{3,n}$, $\hat{\delta}_{1,n}$, $\hat{\delta}_{2,n}$, and $\hat{\delta}_{3,n}$ estimation are shown in Fig. 3, and the convergence property of $\epsilon_{1,n}$ estimation is shown in Fig. 4, for $E_\mathrm{b}/N_0 = 10$ dB, CIR $= -20$ dB, and correction value settings of $(1,1,1),(1,0,1),(1,0,0),(0,0,1)$. In Fig. 3, the estimation accuracy of $\hat{\epsilon}_{2,n}$ is evaluated in terms of the mean square error (MSE), $\mathrm{E}\left[\left|\overline{\hat{\epsilon}}_{2,n} - \hat{\epsilon}_{2,n}\right|^2\right]$. The estimation accuracies of $\hat{\epsilon}_{3,n}$, $\hat{\delta}_{1,n}$, $\hat{\delta}_{2,n}$, and $\hat{\delta}_{3,n}$ are defined similarly. These estimations achieve rapid convergence.

B. BER vs. E_b/N_0

A plot of the bit error rate (BER) vs. E_b/N_0 obtained by changing the correction value settings is shown in Fig. 5, for CIR $= -20$ dB. When the coefficient matrix in (34) is not a regular matrix, the performance is very poor. By setting the correction matrix properly, good performance can be obtained.

C. BER vs. Hilbert Transformer Imperfection

The BER vs. I/Q gain ratio $g_{\mathrm{I},n}/g_{\mathrm{Q},n}$ is shown in Fig. 6, and the BER vs. I/Q phase error ϕ_n is shown in Fig. 7, for $E_\mathrm{b}/N_0 = 10$ dB, CIR $= -20$ dB or -40 dB, and correction value settings of $(1,1,1),(1,0,1),(1,0,0),(0,0,1)$. The proposed receiver can maintain its performance for various I/Q gain ratios or I/Q phase errors.

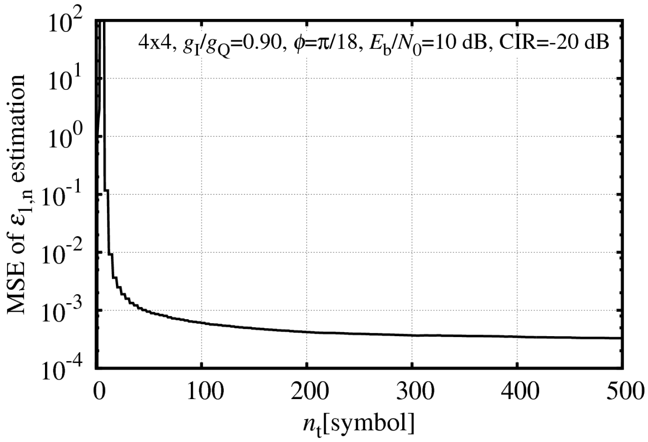

Fig. 4. Convergence property of $\epsilon_{1,n}$ estimation.

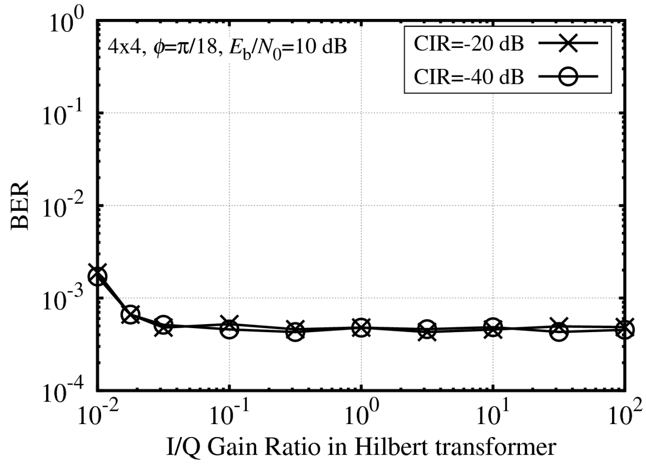

Fig. 6. BER vs. I/Q gain ratio $g_{\mathrm{I},n}/g_{\mathrm{Q},n}$.

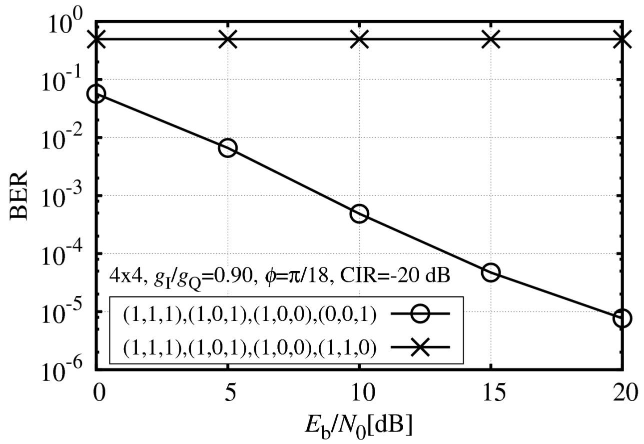

Fig. 5. BER vs. E_b/N_0 obtained by changing the correction value settings.

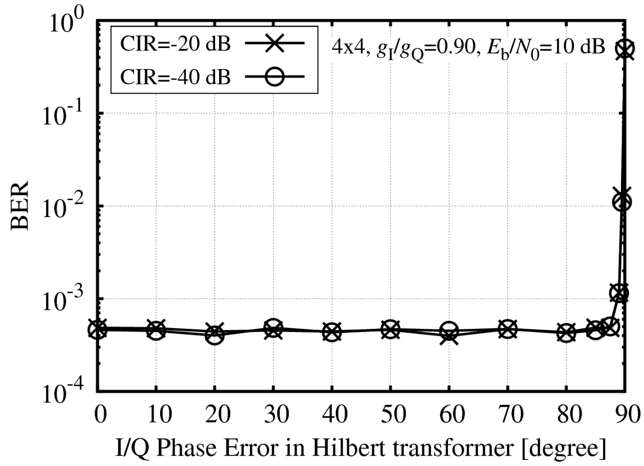

Fig. 7. BER vs. I/Q phase error ϕ_n.

V. Conclusion

This paper proposes a reduced-complexity multiband MIMO receiver with estimation of the analog devices imperfection. By estimating the imperfection of the analog devices in the feedback loop, the proposed receiver can achieve good performance and reduce its computational complexity even in the presence of image-band interference signals.

References

[1] J. Mitra III and C. G. Maguire Jr.,"Cognitive radio: Making software radios more personal," *IEEE Personal Comm. Mag.*, vol. 6, no. 4, pp. 13–18, Aug. 1999.

[2] S. Haykin,"Cognitive radio: Brain-empowered wireless communications," *IEEE J. Select Areas Commun.*, vol. 23, no. 2, pp. 201–220, Feb. 2005.

[3] J. Ryynanen, S. Lindfors, K. Stadius, and K. A.I. Halonen, "Integrated circuits for multi-band multi-mode receivers," *IEEE Circuits and Systems Magazine*, pp. 5–16, 2006.

[4] H. Tsurumi and Y. Suzuki,"Broadband RF stage architecture for software-defined radio in handheld terminal applications," *IEEE Commun. Mag.*, vol. 37, no. 2, pp. 90–95, Feb. 1999.

[5] J. R. Long, "A low-voltage 5.1-5.8-GHz image-reject downconverter RF IC," *IEEE J. Solid-State Circuits*, vol. 35, no. 9, pp. 1320–1328, Sep. 2000.

[6] G. J. Foschini, "Layered space-time architecture for wireless communication in a fading environment when using multi-element antennas," *Bell Labs Tech. Journal*, vol. 1, no. 2, pp. 41–59, Oct. 1996.

[7] G. J. Foschini and M. J. Gans,"On limits of wireless communications in a fading environment when using multiple antennas," *Wireless Pers. Commun.*, vol. 6, no. 3, pp. 311–335, Mar. 1998.

[8] T. Ohta, S. Denno, T. Furuno, and M. Morikura,"A multiband MIMO receiver with ordered successive detection for cognitive radio," *PIMRC'11*, pp. 503–507, Toronto, Sep. 2011.

[9] D. Hayashi, T. Furuno, and S. Denno, "A dual frequency conversion receiver with an adaptive linear image-band interference canceller for multimode/band communications," *PIMRC'07*, Athens, Greece, Sep. 2007.

[10] S. Haykin, Adaptive Filter Theory, 4th ed., Prentice Hall, 1996.